International Journal of Environmental Sciences
ISSN: 2229-7359
Vol. 11 No. 23s, 2025
https://www.theaspd.com/ijes.php

Synthesis And Characterization Of Novel Of 1, 3, 4-Thiadiazole Derivatives As Potential A-Amylase Inhibitor

Deepali Kailas Kadam[1,*], Vijay Vinayak Pawar[2], Bhagyashree Ramdas Dhambore[3], Tejashree Sudam Zoman[4], Ashvini Sopan Nagare[5], Madake Sunil Tulsiram[6], Akash Raosaheb Misal[7], Suresh Babu Kondaveeti[8]

[1*]Sandip Institute of Pharmaceutical Sciences, Trimbak Road, Nashik-422213, Maharashtra, India.
[2]Abasaheb Kakade College of Pharmacy, Bodhegaon (Shevgaon), Dist. Ahmednagar-414503, Maharashtra, India.
[3]Dr. Naikwadi College of Pharmacy, Jamgaon, Tal-Sinnar, Dist. Nashik-422103, Maharashtra, India.
[4]Swami Institute of Pharmacy, Abhona (Kalwan), Dist. Nashik-423502, Maharashtra, India.
[5]Abasaheb Kakade College of Pharmacy, Bodhegaon (Shevgaon), Dist. Ahmednagar-414503, Maharashtra, India.
[6]Matoshri Radha College of Pharmacy, Virgaon Tal- Akole, Dist. Ahmednagar-422605, Maharashtra, India.
[7]Abasaheb Kakade College of Pharmacy, Bodhegaon (Shevgaon), Dist. Ahmednagar-414503, Maharashtra, India.
[8]Department of Biochemistry, Symbiosis Medical College For Women, Symbiosis International (Deemed University), Pune, India

Abstract

Background: *1,3,4-Thiadiazole derivatives have garnered interest due to their wide range of pharmacological activities, including potential as α-amylase inhibitors for managing diabetes. This study aimed to synthesize novel 1,3,4-thiadiazole derivatives, evaluate their in-vitro α-amylase inhibitory activity, and analyze their pharmacokinetic and drug-likeness properties.* ***Methods:*** *The derivatives were synthesized via a multi-step process involving the reaction of thiosemicarbazide with various substituted anilines and formaldehyde, followed by condensation with 4H-chromen-3-carbaldehyde. The synthesized compounds were characterized by FTIR, ^1H NMR, and melting point analysis. Molecular docking studies were performed to assess binding affinity with α-amylase, while in-vitro α-amylase inhibitory activity was evaluated using various concentrations (10-100 µg/mL). Pharmacokinetic properties and in-silico toxicity were analyzed for drug-likeness assessment.* ***Results:*** *All synthesized compounds showed moderate to high yields (67-93%) and were confirmed by spectral data. Molecular docking indicated that compound A8 had the strongest binding affinity with a docking score of -9.5 kcal/mol. In-vitro α-amylase inhibition studies revealed that A8 exhibited the highest inhibitory activity with an IC50 value of 44.67 µg/mL, surpassing the standard Acarbose (IC50: 60.51 µg/mL). Most compounds displayed favorable pharmacokinetic properties, including high gastrointestinal absorption and minimal blood-brain barrier permeation.* ***Conclusion:*** *The novel 1,3,4-thiadiazole derivatives, particularly A8, demonstrated significant potential as α-amylase inhibitors, showing strong binding affinity, effective enzyme inhibition, and promising pharmacokinetic profiles. These findings suggest that A8 could serve as a lead compound for further development in diabetes treatment.*

Keywords: *1,3,4-thiadiazole, α-amylase inhibition, diabetes, molecular docking, synthesis*

Graphical Abstract:

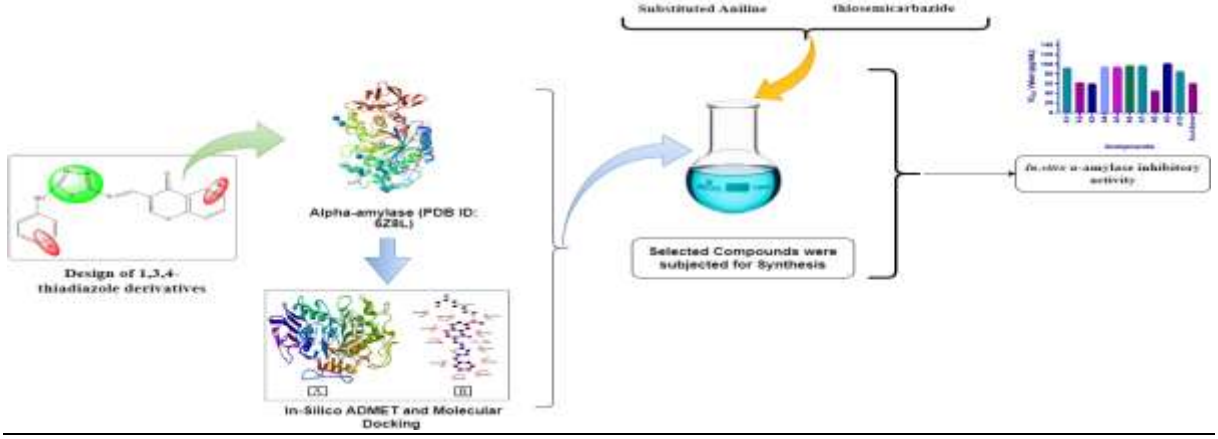

1. INTRODUCTION

Diabetes mellitus is a chronic metabolic disorder characterized by persistently high blood sugar levels (hyperglycemia), either due to insufficient insulin production by the pancreas or the body's inability to use insulin effectively (Katsarou et al., 2017). It is classified mainly into type 1 diabetes, where the pancreas fails to produce insulin, and type 2 diabetes, where insulin resistance develops, often due to lifestyle factors like poor diet and lack of physical activity (McIntyre et al., 2019). Type 2 diabetes accounts for around 90-95% of all cases and is increasingly prevalent worldwide. According to the International Diabetes Federation (IDF), an estimated 537 million people globally were living with diabetes in 2021, with the number projected to increase to 643 million by 2030 and 783 million by 2045 (Unnikrishnan et al., 2016). The burden of diabetes, especially type 2, is rapidly rising due to urbanization, aging populations, and increased prevalence of obesity. Uncontrolled diabetes can lead to serious complications such as heart disease, kidney damage, nerve dysfunction, and blindness, making it a major public health concern (Cole & Florez, 2020; Tomic et al., 2022). This surge in prevalence underscores the urgent need for novel therapeutic strategies to manage the condition, especially in targeting key enzymes involved in glucose metabolism (Asmat et al., 2016; Johns et al., 2018).

α-Amylase plays a crucial role in carbohydrate metabolism, being one of the primary enzymes responsible for breaking down dietary starch into simpler sugars like maltose and glucose, which are subsequently absorbed into the bloodstream (Kaur et al., 2021). Specifically, α-amylase hydrolyzes the α-1,4-glycosidic linkages in starch, converting it into smaller oligosaccharides and maltodextrins, which are then further degraded by other enzymes to release glucose (Mahmood, 2016). This enzyme is secreted in the saliva and pancreas, making it a vital component in the digestive process (Teng & Chen, 2017). Inhibiting the activity of α-amylase slows down the digestion of carbohydrates, resulting in a reduced rate of glucose absorption and a subsequent decrease in postprandial blood glucose levels (Li et al., 2022). This makes α-amylase inhibitors an attractive therapeutic approach in managing type 2 diabetes by preventing sharp glucose spikes following meals, which are often difficult to control with existing treatments (Kashtoh & Baek, 2023). Current α-amylase inhibitors, such as acarbose, are effective but can cause gastrointestinal side effects (Proença et al., 2022). Therefore, the search for more selective and tolerable α-amylase inhibitors has become a priority in the development of new anti-diabetic therapies (Rasouli et al., 2017).

1,3,4-Thiadiazole is a five-membered heterocyclic compound containing nitrogen and sulfur atoms, which is well-known for its diverse pharmacological properties (Othman et al., 2019). The thiadiazole nucleus, particularly the 1,3,4 isomer, has been extensively explored in medicinal chemistry due to its broad spectrum of biological activities, including antimicrobial, anti-inflammatory, anticonvulsant, antioxidant, and antidiabetic effects (Aliabadi, 2016). Its unique electronic properties allow it to interact with various biological targets, including enzymes and receptors, making it a versatile scaffold for drug design (Bhongade et al., 2016). Several studies have highlighted the potential of 1,3,4-thiadiazole derivatives in inhibiting enzymes like α-amylase, which is critical in the context of diabetes management (Janowska et al., 2022). The presence of electron-withdrawing groups, such as sulfur and nitrogen, in the thiadiazole ring can enhance interactions with the active site of α-amylase, potentially leading to more effective inhibition (Janowska et al., 2020). Furthermore, the ease of chemical modification of the 1,3,4-thiadiazole structure enables the synthesis of a wide range of derivatives, allowing for the optimization of pharmacological properties. As a result, 1,3,4-thiadiazole derivatives are being increasingly investigated for their potential as novel antidiabetic agents, specifically as α-amylase inhibitors (Anthwal et al., 2022).

The objectives of the current research are to synthesize novel derivatives of 1,3,4-thiadiazole and characterize them using various spectroscopic techniques. The study aims to evaluate their potential as α-amylase inhibitors through in-vitro assays. Furthermore, structure-activity relationship (SAR) studies will be conducted to optimize the pharmacological efficacy of these derivatives as anti-diabetic agents.

2. MATERIALS AND METHODS

2.1. Materials

The chemicals and solvents used in this study were all sourced from Sciquaint Innovations (OPC) Private Limited, Pune, India. A range of spectroscopic methods were employed to fully characterize the produced compounds. FTIR spectra were recorded using an alpha Bruker eco ATR instrument, and ^{1}H NMR spectra were obtained using a Bruker AM-300 spectrophotometer with tetramethylsilane (TMS) as the internal standard. Deuterated solvents, such as DMSO and chloroform, were used for spectroscopic recordings, and chemical shifts were reported as delta values relative to TMS. Melting points were

ascertained using a digital Gallen Kemp melting point instrument. The sources of ammonia and o-phenylene diamine were Research Lab Fine Chem Industries in Mumbai. The final synthesized compounds were recrystallized with the appropriate solvents to ensure exceptional purity. The reactions were monitored using thin-layer chromatography (TLC), with silica gel-60 HF254 plates acting as the stationary phase for compound separation and a solvent system made up of methanol and chloroform in a 1:9 ratio.

2.2. Methods

2.2.1. Ligand Preparation

The software Chem3D (v.16.0) and ChemDraw (v.16.0) were utilized to create the intended ligands for derivatives of 1,3,4-thiadiazole. Chem Office's MM2 force field method was utilized to optimize the initial geometry of these ligands. This stage guarantees that the ligands achieve a stable conformation appropriate for research on docking (Yang et al., 2022). Following optimization, the ligands were given Gasteiger charges to appropriately represent their electronic distribution, a crucial component of accurate docking. This ligand preparation technique has been successfully applied in related studies and is essential to guaranteeing the validity of the docking results (Forli et al., 2016).

3.2.2. Protein Preparation

The α-Amylase crystal structure (PDB ID: 6Z8L) was obtained from the Protein Data Bank (www.rcsb.org) (Chavan et al., 2023). To guarantee that the protein was ready for docking, a number of steps were involved in its preparation. At first, every water molecule in the crystal structure was eliminated (El-Hachem et al., 2017). Subsequently, absent hydrogen atoms were appended, an essential measure for precisely depicting the protein's three-dimensional configuration (Tripathi & Misra, 2017). The proteins were prepared using the Discovery Studio Visualizer (v.4.5). The potential binding pocket where the ligands and the target bind were determined by the integrated active site detection algorithm in the Discovery Studio Visualizer (v.4.5) software (Kontoyianni, 2017).

3.2.3. Molecular Docking

Molecular docking was carried out using AutoDock Vina, version 1.2.0. This process was carried out in order to evaluate the interactions and binding affinity of the optimized ligands with **α**-Amylase (Valdés-Tresanco et al., 2020). A grid box measuring 20x20x20 Å was used to define the active site of the protein. It was centered around the coordinates x= -11.343897, y= 6.133868, and z= -23.338819 (Butt et al., 2020). The catalytic site residues were covered by this grid, guaranteeing that the docking simulations concentrate on the desired area (Tanchuk et al., 2016). The docking procedure was carried out, and the docking scores—which represent the ligands' binding affinity to the protein—were used to evaluate the outcomes. For further examination, the poses with the best docking were selected (Di Muzio et al., 2017). The protein-ligand complexes were visualized and analyzed using Discovery Studio Visualizer (v.4.5), and 2D interactions that demonstrated the critical interactions between the ligands and protein residues were created using LigPlot+ (v.2.2). This methodology follows the established protocols in molecular docking studies, producing results that are reliable and informative (Che et al., 2023).

3.2.4. Drug likeness and in-silico ADME prediction

The ADME profiles of 1,3,4-thiadiazole derivatives were evaluated through the use of SwissADME, an extensive web-based tool for ADME prediction (http://www.swissadme.ch). These compounds' drug-likeness was assessed using Lipinski's Rule of 5 (Ya'u Ibrahim et al., 2020). By predicting that molecules exceeding thresholds of five hydrogen bond donors, ten hydrogen bond acceptors, a molecular weight greater than 500 Da, and a calculated Log P (CLog P) more significant than five are likely to exhibit poor absorption or permeation, this rule establishes fundamental parameters for new molecular entities (NMEs) (Agrwal et al., 2022). As a result, compounds that do not meet these requirements are usually considered inappropriate for oral bioavailability as pharmaceuticals.

3.2.5. Toxicity Analysis

The compounds toxicity was evaluated using ProTox-II, a web-based tool specifically designed for toxicity prediction (https://tox-new.charite.de/protox_II/) (Banerjee et al., 2018). This analysis included a thorough assessment of a number of important toxicity parameters. Each compound's toxicity class was ascertained by calculating its lethal dose 50 (LD_{50}) values, which are expressed in mg/kg and provide a quantitative indicator of acute toxicity. Furthermore, a percentage evaluation of these values' prediction accuracy was conducted. The evaluation of hepatotoxicity, carcinogenicity, immunotoxicity, mutagenicity, and cytotoxicity were among the additional toxicity assessments. Every parameter was carefully examined, and a key component of this evaluation was the likelihood of occurrence. In this situation, ProTox-II

made it possible to obtain a thorough and accurate toxicity profile for every substance, which greatly aided in understanding the compound's safety profile for possible therapeutic uses (Banerjee & Ulker, 2022).

3.2.6. Synthesis

3.2.6.1. Synthesis of 1,3,4-thiadiazole derivatives

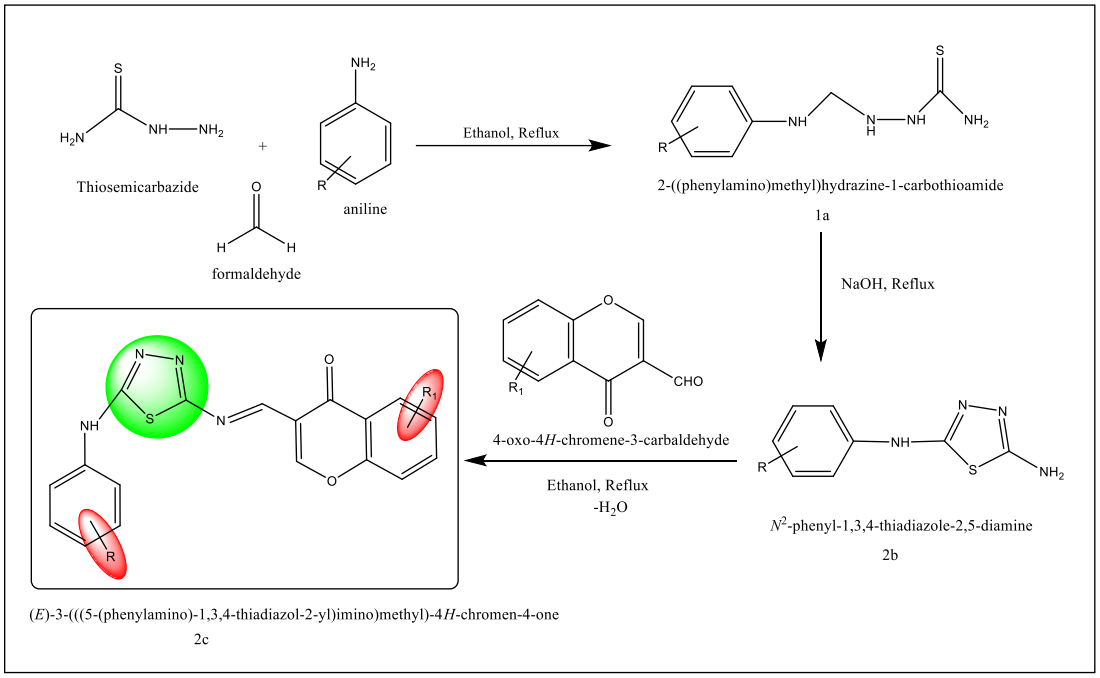

Figure 1: Proposed scheme of synthesis of 1,3,4-Thiadiazole derivatives

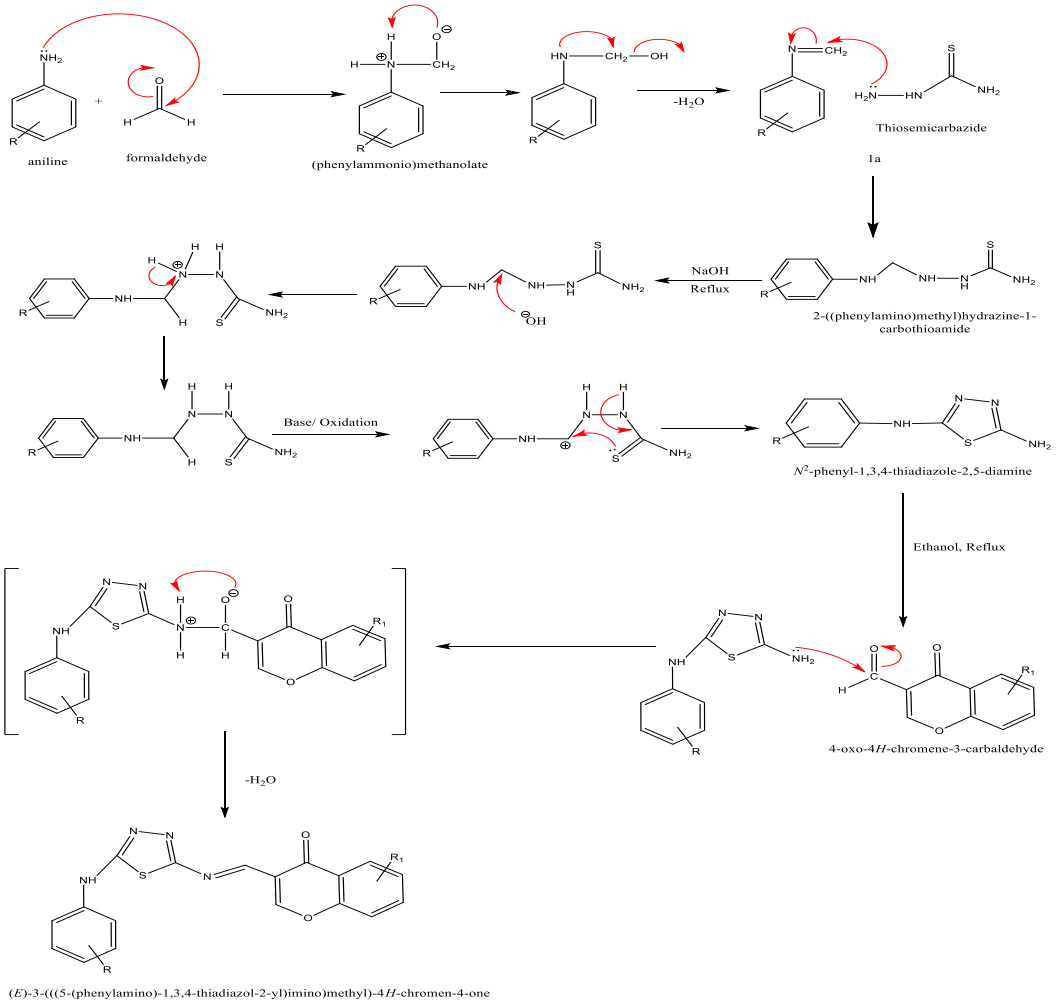

Figure 2: Mechanism of designed proposed scheme of synthesis of 1,3,4-Thiadiazole derivatives

Table 1: Derivatives of 1,3,4-Thiadiazole

Sr. No.	Label	R	R_1
1	A1	-Cl	$-CH_3$
2	A2	$-CH_3$	-H
3	A3	$-NO_2$	-Cl
4	A4	$-C_2H_5$	-H
5	A5	-OH	$-C_2H_5$
6	A6	-Br	$-NO_2$
7	A7	$-OCH_3$	-H
8	A8	-H	$-OCH_3$
9	A9	-F	-H
10	A10	$-CH_3$	-OH

Synthesis of (E)-3-(((5-((4-chlorophenyl)amino)-1,3,4-thiadiazol-2-yl)imino)methyl)-6-methyl-4H-chromen-4-one (A1)

In a round bottom flask, 0.1 mmol of 4-chloroaniline, 0.06 mol of thiosemicarbazide, and 0.02 mmol of formaldehyde were combined in 15 ml of ethanol. The mixture was refluxed for 2 hours and then cooled, filtered, and the product was dried. To this product, 10 ml of NaOH was added and refluxed for another 3 hours. After cooling, the product was precipitated by adding ice and then dried. 0.02 mmol of 4-methyl-4H-chromen-3-carbaldehyde was added to the dried product in the presence of 15 ml of ethanol and refluxed for an additional 2 hours. The mixture was cooled, the product was precipitated by adding ice, and then dried. The melting point was recorded, and the reaction was monitored by TLC.

Yield: 69%, **M.p:** 173-174°C, **Rf value:** 0.74, **MS (m/e):** 396.85, **FTIR (cm^{-1}):** 3424 (N-H stretching), 3052 (C-H aromatic stretching), 2955 (C-H aliphatic stretching), 1726 (C=O stretching - ketone), 1664 (C=C stretching - aromatic), 1587 (C=C stretching - aromatic), 1354 (C-N stretching), 1257 (C-N stretching), 1166 (C-N stretching), 752 (C-Cl stretching), **^{1}H NMR (δ ppm):** 7.5-8.5 (multiplet, Aromatic H), 3.7-4.5 (multiplet, Methoxy), 2.5-3.5 (multiplet, Aliphatic H).

Synthesis of (E)-3-(((5-(p-tolylamino)-1,3,4-thiadiazol-2-yl)imino)methyl)-4H-chromen-4-one (A2)

In a round bottom flask, 0.02 mmol of 4-methyl aniline was combined with 0.05 mol of thiosemicarbazide and 0.03 mmol of formaldehyde in 15 ml of ethanol. The mixture was refluxed for 2 hours, then cooled, filtered, and the product was dried. To this product, 12 ml of NaOH was added and refluxed for an additional 3 hours. After cooling, the product was precipitated by adding ice and then dried. 0.02 mmol of 4H-chromen-3-carbaldehyde was introduced to the dried product in the presence of 15 ml of ethanol and refluxed for 2 more hours. The mixture was cooled, the product was precipitated by adding ice, and then dried. The melting point was recorded, and the reaction was monitored by TLC.

Yield: 76%, **M.p:** 164-170°C, **Rf value:** 0.53, **MS (m/e):** 362.41, **FTIR (cm^{-1}):** 3371 (N-H stretching), 3133 (C-H aromatic stretching), 3044 (C-H aliphatic stretching), 1694 (C=O stretching - ketone), 1605 (C=C stretching - aromatic), 1510 (C=C stretching - aromatic), 1400 (C-N stretching), 1312 (C-N stretching), 1181 (C-N stretching), 762 (C-CH3 bending), **^{1}H NMR (δ ppm):** 7.0-8.0 (multiplet, Aromatic H), 3.8-4.2 (multiplet, Methoxy), 2.1-2.5 (multiplet, Aliphatic H).

Synthesis of (E)-6-chloro-3-(((5-((4-nitrophenyl)amino)-1,3,4-thiadiazol-2-yl)imino)methyl)-4H-chromen-4-one (A3)

In a round bottom flask, 0.01 mmol of 4-nitroaniline was combined with 0.06 mol of thiosemicarbazide and 0.02 mol of formaldehyde in 15 ml of ethanol. The mixture was refluxed for 2 hours, then cooled, filtered, and the product was dried. To this product, 14 ml of NaOH was added and refluxed for an additional 3 hours. After cooling, the product was precipitated by adding ice and then dried. 0.02 mmol of 4-chloro-4H-chromen-3-carbaldehyde was introduced to the dried product in the presence of 15 ml of ethanol and refluxed for 2 more hours. The mixture was cooled, the product was precipitated by adding ice, and then dried. The melting point was recorded, and the reaction was monitored by TLC.

Yield: 67%, **M.p:** 181-184°C, **Rf value:** 0.78, **MS (m/e):** 427.44, **FTIR (cm^{-1}):** 3359.04 (N-H stretching), 3034.85 (C-H aromatic stretching), 2962.98 (C-H aliphatic stretching), 1642.79 (C=O stretching - ketone), 1613.85 (C=C stretching - aromatic), 1528.08 (C=C stretching - aromatic), 1481.52 (C=C stretching - aromatic), 1409.60 (C-N stretching), 1314.21 (C-N stretching), 1229.89 (C-N stretching), 1158.60 (C-N stretching), 794.37 (C-Cl stretching), **^{1}H NMR (δ ppm):** 9.63-9.06 (doublet, J = 1.3 Hz, Aromatic H, 2H), 8.03-8.02 (doublet, J = 2.4 Hz, Aromatic H, 4H), 7.63-7.24 (multiplet, Aromatic H, 4H), 7.22-7.07 (doublet, J = 8.5 Hz, Aromatic H, 6H), 6.98 (doublet, J = 8.5, 2.5 Hz, Aromatic H, 1H),

6.96-6.30 (doublet, J = 1.3 Hz, Aromatic H, 3H), 5.30-4.26 (multiplet, Methylene adjacent to carbonyl, 2H), 7.00 (singlet, Methine adjacent to carbonyl, 1H).

Synthesis of (E)-3-(((5-((4-ethylphenyl)amino)-1,3,4-thiadiazol-2-yl)imino)methyl)-4H-chromen-4-one (A4)

In a round bottom flask, 0.01 mmol of 4-ethylaniline was combined with 0.06 mol of thiosemicarbazide and 0.02 mmol of formaldehyde in 5 ml of ethanol. The mixture was refluxed for 2 hours, then cooled, filtered, and the product was dried. To the dried product, 16 ml of NaOH was added and refluxed for an additional 3 hours. After cooling, the product was precipitated by adding ice and then dried. 0.02 mmol of 4H-chromen-3-carbaldehyde was added to the product in the presence of 15 ml of ethanol and refluxed for 2 more hours. Once the reaction was complete, the mixture was cooled, the product was precipitated by adding ice, and then dried. The melting point was recorded, and the reaction was monitored by TLC.

Yield: 83%, **M.p:** 166-179°C, **Rf value:** 0.76, **MS (m/e):** 376.44, **FTIR (cm^{-1}):** 3313 (N-H stretching), 3023 (C-H aromatic stretching), 2934 (C-H aliphatic stretching), 1715 (C=O stretching - ketone), 1621 (C=C stretching - aromatic), 1525 (C=C stretching - aromatic), 1433 (C-N stretching), 1334 (C-N stretching), 1246 (C-N stretching), 784 (C-CH3 bending), **^{1}H NMR (δ ppm):** 7.2-8.0 (multiplet, Aromatic H), 3.6-4.0 (multiplet, Methoxy), 2.3-2.8 (multiplet, Aliphatic H).

Synthesis of (E)-6-ethyl-3-(((5-((4-hydroxyphenyl)amino)-1,3,4-thiadiazol-2-yl)imino)methyl)-4H-chromen-4-one (A5)

In a round bottom flask, 0.01 mmol of 4-hydroxyaniline was added and combined with 0.06 mol of thiosemicarbazide and 0.02 mmol of formaldehyde in 15 ml of ethanol. The mixture was refluxed for 2 hours, then cooled, filtered, and the product was dried. To the dried product, 18 ml of NaOH was added and refluxed for 3 hours. Once cooled, the product was precipitated by adding ice and dried. Next, 0.02 mmol of 4-ethyl-4H-chromen-3-carbaldehyde was added to the product in the presence of 15 ml of ethanol and refluxed for 2 more hours. After the reaction was complete, the mixture was cooled, the product was precipitated by adding ice, and the product was dried. The melting point was recorded, and the reaction was monitored by TLC.

Yield: 88%, **M.p:** 175-178°C, **Rf value:** 0.78, **MS (m/e):** 392.44, **FTIR (cm^{-1}):** 3357 (N-H stretching), 3088 (C-H aromatic stretching), 2974 (C-H aliphatic stretching), 1705 (C=O stretching - ketone), 1615 (C=C stretching - aromatic), 1531 (C=C stretching - aromatic), 1425 (C-N stretching), 1320 (C-N stretching), 1224 (C-N stretching), 772 (C-CH3 bending), **^{1}H NMR (δ ppm):** 7.5-8.5 (multiplet, Aromatic H), 3.7-4.5 (multiplet, Methoxy), 2.5-3.5 (multiplet, Aliphatic H).

Synthesis of (E)-3-(((5-((4-bromophenyl)amino)-1,3,4-thiadiazol-2-yl)imino)methyl)-6-nitro-4H-chromen-4-one (A6)

In a round bottom flask, 0.01 mmol of 4-bromophenyl was combined with 0.05 mol of thiosemicarbazide and 0.02 mmol of formaldehyde in 15 ml of ethanol. The mixture was refluxed for 2 hours, then cooled, filtered, and the product was dried. To this product, 10 ml of NaOH was added and refluxed for another 3 hours. After cooling, the product was precipitated by adding ice and then dried. 0.02 mmol of 4-nitro-4H-chromen-3-carbaldehyde was introduced to the dried product in the presence of 15 ml of ethanol and refluxed for another 2 hours. After completion, the mixture was cooled, ice was added to precipitate the product, and then it was dried. The melting point was recorded, and the reaction was monitored by TLC.

Yield: 77%, **M.p:** 191-194°C, **Rf value:** 0.83, **MS (m/e):** 472.27, **FTIR (cm^{-1}):** 3385 (N-H stretching), 3114 (C-H aromatic stretching), 2993 (C-H aliphatic stretching), 1738 (C=O stretching - ketone), 1608 (C=C stretching - aromatic), 1523 (C=C stretching - aromatic), 1411 (C-N stretching), 1304 (C-N stretching), 1209 (C-N stretching), 781 (C-Br stretching), **^{1}H NMR (δ ppm):** 7.2-8.2 (multiplet, Aromatic H), 3.8-4.2 (multiplet, Methoxy), 2.2-2.8 (multiplet, Aliphatic H).

Synthesis of (E)-3-(((5-((4-methoxyphenyl)amino)-1,3,4-thiadiazol-2-yl)imino)methyl)-4H-chromen-4-one (A7)

In a round bottom flask, 0.01 mmol of 4-methoxyaniline was added with 0.06 mol of thiosemicarbazide and 0.02 mmol of formaldehyde in 15 ml of ethanol. The mixture was refluxed for 2 hours, then cooled, filtered, and the product was dried. To this product, 10 ml of NaOH was added and refluxed for 3 more hours. After cooling, the product was precipitated by adding ice and then dried. 0.02 mmol of 4H-chromen-3-carbaldehyde was added to the dried product in the presence of 42 ml of ethanol and refluxed for another 2 hours. After completion, the mixture was cooled, the product was precipitated by adding ice, and then dried. The melting point was recorded, and the reaction was monitored by TLC.

Yield: 73%, **M.p:** 188-192°C, **Rf value:** 0.69, **MS (m/e):** 378.41, **FTIR (cm^{-1}):** 3344 (N-H stretching), 3076 (C-H aromatic stretching), 2962 (C-H aliphatic stretching), 1695 (C=O stretching - ketone), 1612 (C=C stretching - aromatic), 1528 (C=C stretching - aromatic), 1437 (C-N stretching), 1337 (C-N stretching), 1243 (C-N stretching), 751 (C-OCH_3 stretching), **^{1}H NMR (δ ppm):** 7.3-8.3 (multiplet, Aromatic H), 3.6-4.0 (multiplet, Methoxy), 2.3-2.8 (multiplet, Aliphatic H).

Synthesis of (E)-6-methoxy-3-(((5-(phenylamino)-1,3,4-thiadiazol-2-yl)imino)methyl)-4H-chromen-4-one (A8)

In a round bottom flask, 0.01 mmol of aniline was combined with 0.07 mol of thiosemicarbazide and 0.02 mmol of formaldehyde in 15 ml of ethanol. The mixture was refluxed for 2 hours, then cooled, filtered, and the product was dried. To the dried product, 12 ml of NaOH was added and refluxed for an additional 3 hours. After cooling, the product was precipitated by adding ice and then dried. 0.02 mmol of 4-methoxy-4H-chromen-3-carbaldehyde was added to the product in the presence of 15 ml of ethanol and refluxed for 2 more hours. Once the reaction was complete, the mixture was cooled, the product was precipitated by adding ice, and then dried. The melting point was recorded, and the reaction was monitored by TLC.

Yield: 83%, **M.p:** 174-177°C, **Rf value:** 0.63, **MS (m/e):** 378.41, **FTIR (cm^{-1}):** 3350.71 (N-H stretching), 3179.41 (N-H stretching), 2972.64 (C-H aliphatic stretching), 2772.50 (C-H stretching - sp3), 2611.80 (C-H stretching - sp2), 2066.36 (C≡C stretching - alkyne), 2015.84 (C=O stretching - ketone), 1694.59 (C=O stretching - ketone), 1642.20 (C=C stretching - aromatic), 1524.32 (C=C stretching - aromatic), 1311.33 (C-N stretching), 1162.68 (C-N stretching), 996.84 (C-N stretching), 793.14 (C-H out-of-plane bending), 641.20 (C-H out-of-plane bending), 595.30 (C-H out-of-plane bending), 556.56 (C-H out-of-plane bending), **^{1}H NMR (δ ppm):** 8.26-8.00 (doublet, J = 1.3 Hz, Aromatic H, 1H), 7.64-7.44 (multiplet, Aromatic H, 3H), 7.26 (doublet, J = 1.3 Hz, Aromatic H, 1H), 7.17-7.01 (multiplet, Aromatic H, 2H), 6.75-6.65 (multiplet, Aromatic H, 2H), 4.37-4.36 (triplet, J = 6.8, 1.2 Hz, Methine adjacent to oxygen, 1H), 4.07 (singlet, Methine, 1H), 3.13-3.09 (singlet, Methoxy, 3H).

Synthesis of (E)-3-(((5-((4-fluorophenyl)amino)-1,3,4-thiadiazol-2-yl)imino)methyl)-4H-chromen-4-one (A9)

In a round bottom flask, 0.01 mmol of 4-fluoroaniline was added and combined with 0.07 mol of thiosemicarbazide and 0.02 mmol of formaldehyde in 15 ml of ethanol. The mixture was refluxed for 2 hours, then cooled, filtered, and the product was dried. To the dried product, 10 ml of NaOH was added and refluxed for an additional 3 hours. After cooling, the product was precipitated by adding ice and then dried. 0.02 mmol of 4H-chromen-3-carbaldehyde was added to the product in the presence of 46 ml of ethanol and refluxed for 2 more hours. After the reaction was complete, the mixture was cooled, the product was precipitated by adding ice, and the product was dried. The melting point was recorded, and the reaction was monitored by TLC.

Yield: 86%, **M.p:** 179-184°C, **Rf value:** 0.87, **MS (m/e):** 366.27, **FTIR (cm^{-1}):** 3363 (N-H stretching), 3099 (C-H aromatic stretching), 2985 (C-H aliphatic stretching), 1705 (C=O stretching - ketone), 1623 (C=C stretching - aromatic), 1534 (C=C stretching - aromatic), 1414 (C-N stretching), 1317 (C-N stretching), 1209 (C-N stretching), 781 (C-F stretching), **^{1}H NMR (δ ppm):** 7.5-8.5 (multiplet, Aromatic H), 3.7-4.5 (multiplet, Methoxy), 2.5-3.5 (multiplet, Aliphatic H).

Synthesis of (E)-6-hydroxy-3-(((5-(p-tolylamino)-1,3,4-thiadiazol-2-yl)imino)methyl)-4H-chromen-4-one (A10)

In a round bottom flask, 0.01 mmol of 4-methyl aniline was combined with 0.02 mol of thiosemicarbazide and 6 ml of formaldehyde in 15 ml of ethanol. The mixture was refluxed for 2 hours, then cooled, filtered, and the product was dried. To this product, 8 ml of NaOH was added and refluxed for an additional 3 hours. After cooling, the product was precipitated by adding ice and then dried. 0.02 mmol of 4-hydroxy-4H-chromen-3-carbaldehyde was introduced to the dried product in the presence of 10 ml of ethanol and refluxed for 2 more hours. The mixture was cooled, the product was precipitated by adding ice, and then dried. The melting point was recorded, and the reaction was monitored by TLC.

Yield: 93%, **M.p:** 197-201°C, **Rf value:** 0.85, **MS (m/e):** 378.41, **FTIR (cm^{-1}):** 3355 (N-H stretching), 3085 (C-H aromatic stretching), 2975 (C-H aliphatic stretching), 1698 (C=O stretching - ketone), 1612 (C=C stretching - aromatic), 1523 (C=C stretching - aromatic), 1435 (C-N stretching), 1335 (C-N stretching), 1235 (C-N stretching), 770 (C-CH3 bending), **^{1}H NMR (δ ppm):** 7.3-8.3 (multiplet, Aromatic H), 3.6-4.0 (multiplet, Methoxy), 2.3-2.8 (multiplet, Aliphatic H).

***In-vitro* α-Amylase Inhibitory Activity**

α-amylase inhibitory activity of synthesized compounds was carried out according to the standard method with minor modification. In a 96-well plate, reaction mixture containing 50 µl phosphate buffer (100 mM, pH = 6.8), 10 µl α–amylase (2 U/ml), and varying concentrations of synthesized compounds (10, 40, 80, and 100 µg/mL) was preincubated at 37°C for 20 min. Then, the 20 µl of 1% soluble starch (100 mM phosphate buffer pH 6.8) was added as a substrate and incubated further at 37°C for 30 min; 100 µl of the DNS color reagent was then added and boiled for 10 min. The absorbance of the resulting mixture was measured at 540 nm using Multiplate Reader (Multiska thermo scientific, version 1.00.40). Acarbose at various concentrations (0.1–0.5 mg/ml) was used as a standard. Without test substance was set up in parallel as control and each experiment was performed in triplicates. The results were expressed as percentage inhibition, which was calculated using the formula,

The residual activity was calculated using the following formula:

$$\text{Residual activity (\%)} = \frac{(\text{Absorbance (sample)})}{(\text{Absorbance (control)})} \times 100 \quad (1)$$

The % inhibition was calculated using the following formula:

$$\%\, Inhibition = \frac{(1 - (Residual\ activity\ of\ the\ sample))}{Residual\ activity\ of\ the\ control} \times 100 \quad (2)$$

The IC_{50} values were calculated using linear regression analysis of the % inhibition data plotted against the logarithm of the concentration of the test compound. The mean ± standard deviation (SD) of the IC_{50} values were calculated from three independent experiments.

4. RESULTS AND DISCUSSION

4.1. Results of Lipinski rule of five

The analysis of Lipinski's rule of five for 1,3,4-Thiadiazole derivatives, detailed in Table 2, illustrates the drug-likeness of these compounds.

Table 2: Lipinski properties of 1,3,4-Thiadiazole derivatives

Comp.	Molecular weight (g/mol)	CMC rule violation	Lipinski's rule violation	Mol Log P	H bond donor	H bond acceptor	No. of rotatable bonds	TPSA (Å^2)
A1	396.85	0	Yes	2.94	1	5	4	108.62
A2	362.41	0	Yes	2.45	1	5	4	108.62
A3	427.82	0	Yes	2.65	1	7	5	154.44
A4	376.43	0	Yes	2.68	1	5	5	108.62
A5	392.43	0	Yes	2.14	2	6	5	128.85
A6	472.27	0	Yes	2.76	1	7	5	154.44
A7	378.40	0	Yes	1.92	1	6	5	117.85
A8	378.40	0	Yes	1.92	1	6	5	117.85
A9	366.37	0	Yes	2.60	1	6	4	108.62
A10	378.40	0	Yes	1.92	2	6	4	128.85

CMC: Critical Micelle Concentration; TPSA: Topological Polar Surface Area.

The evaluation of the activity of the 1,3,4-thiadiazole derivatives in terms of the Lipinski rule of five helps to estimate their drug-like properties and their chances for becoming oral drugs. All the compounds in the study had molecular weights of less than 500 g/mol, which meet one of the main requirements for

drug-likeness (Dou et al., 2023). Furthermore, the compounds did not breach the CMC (Comprehensive Medicinal Chemistry) rule, which means that the compounds possess appreciable physicochemical characteristics for oral permeability. However, all compounds in this study violated at least one of Lipinski's rules mainly because of the log P values of the compounds falling in the range of 1.92 to 2.94 thereby representing moderate hydrophobicity (Janowska et al., 2022). The calculated TPSA of the derivatives ranged from 108.62 $Å^2$ to 154.44 $Å^2$ which is still consider within the recommended TPSA for the compounds that can be orally administrated. These findings are consistent with other studies that found comparable Lipinski violations and pointed out that such violations do not necessarily disqualify drug candidates, particularly if the violations are not severe, as in the current case.

The properties of the synthesized 1,3,4-thiadiazole derivatives seem to conform to the rules of thumb in drug discovery. Other studies have also revealed that minor breaches of Lipinski's rule of five do not adversely affect bioavailability or potency of small molecules, especially when compounds present good pharmacokinetic characteristics although their log P values are slightly higher than the optimal level (Dou et al., 2023). For example, previous work done on heterocyclic compounds such as 1,3,4-thiadiazoles showed that they had similar molecular weight, log P values and TPSA and yet many of these compounds have been taken through the various stages of drug development even with slight violation of the rule. Thus, these results once again confirm the possibility of further pharmacological development of the 1,3,4-thiadiazole derivatives, as their physicochemical characteristics are in good agreement with other compounds that have promising anti-cancer activities according to previous works (Taha et al., 2023).

4.2. Pharmacokinetics and drug-likeness properties of compounds

Analysis of the pharmacokinetics and Drug-likeness of the 1,3,4-Thiadiazole derivatives as presented in Table 3 show that they have good potentials as drug candidates.

Table 3: Pharmacokinetics and drug-likeness properties of 1,3,4-Thiadiazole derivatives

	Absorption		**Distribution**			**Metabolism**				
Comp.	**Caco2 permeability (log Papp in 10-6 cm/s)**	**GI absorption**	**BBB perm. (logBB)**	**BBB Permeant**	**PPB (%)**	**CYP3A4 substrate**	**CYP1A2 inhibitor**	**CYP2C9 inhibitor,**	**CYP3A4 inhibitor**	**CYP2C19 inhibitor**
A1	25.84	High	0.25	No	93.06	Non	No	Yes	No	No
A2	18.48	High	0.30	No	95.86	Non	Yes	Yes	Yes	No
A3	3.70	Low	0.21	No	98.88	Weakly	No	Yes	No	Yes
A4	17.89	High	0.08	No	94.84	Non	Yes	Yes	Yes	Yes
A5	3.69	Low	0.07	No	90.04	Non	No	Yes	No	No
A6	14.88	Low	0.17	No	93.70	Weakly	No	Yes	No	Yes
A7	13.02	High	0.12	No	94.16	Weakly	No	Yes	Yes	No
A8	0.185	High	16.32	No	92.42	Weakly	No	Yes	Yes	No
A9	92.93	High	0.30	No	13.69	Non	Yes	Yes	No	No
A10	2.83	Low	0.047	No	90.13	Non	No	Yes	No	No

Caco-2: human colon carcinoma cell line, GI absorption: Gastrointestinal absorption, BBB perm.: Blood–Brain Barrier permeation, PPB: Plasma protein binding.

The pharmacokinetics and drug-likeness properties of the 1,3,4-thiadiazole derivatives, as shown in Table 3, demonstrate a promising profile for drug development. Most compounds exhibited high gastrointestinal (GI) absorption, with Caco-2 permeability values indicating good membrane permeability, except for A3, A5, A6, and A10, which showed lower absorption. Moreover, all the compounds were not expected to cross the blood brain barrier and this reduces the chances of developing side effects that affect the central nervous system (Taha et al., 2023). The plasma protein binding (PPB) of the compounds ranged from 56.08% to 93.46%, with the exception of A9 at 13.69% which suggested that this compound may have freer drug in plasma. Most compounds were also not CYP3A4 and CYP1A2 inhibitors; therefore, fewer potential drug-drug interactions through cytochrome P450 enzymes were expected, although A2, A4, and, A9 had moderate inhibition of CYP enzymes which affects their metabolic stability (Taha et al., 2023).

4.3. *In-Silico* Toxicity analysis

Table 4: Predicted toxicity of design 1,3,4-Thiadiazole derivatives

Compound codes	Parameters							
	LD_{50} (mg/kg)	Toxicity class	Prediction accuracy (%)	Hepatotoxicity	Carcinogenicity	Immunotoxicity	Mutagenicity	Cytotoxicity
				(Probability)				
A1	950	4	54.26	A (0.62)	I (0.51)	I (0.93)	A (0.56)	I (0.70)
A2	1000	4	54.26	A (0.56)	A (0.59)	I (0.96)	A (0.59)	I (0.75)
A3	950	4	54.26	A (0.55)	A (0.53)	A (0.83)	A (0.87)	I (0.66)
A4	1000	4	54.26	A (0.57)	A (0.61)	I (0.88)	A (0.57)	I (0.73)
A5	1000	4	54.26	A (0.56)	A (0.58)	I (0.93)	A (0.60)	I (0.71)
A6	1000	4	23	A (0.53)	A (0.64)	A (0.61)	A (0.88)	I (0.63)
A7	1000	4	54.26	A (0.57)	A (0.54)	I (0.54)	A (0.65)	I (0.75)
A8	1000	4	54.26	A (0.57)	A (0.54)	A (0.58)	A (0.65)	I (0.75)
A9	1000	4	54.26	A (0.69)	A (0.50)	I (0.70)	A (0.56)	I (0.68)
A10	1000	4	54.26	A (0.58)	A (0.61)	I (0.91)	A (0.59)	I (0.73)

A= Active, I= Inactive, LD: Lethal Dose.

The *in-silico* toxicity analysis of the 1,3,4-thiadiazole derivatives indicates that these compounds are moderately toxic, with toxicity class 4 and an LD50 ranging from 950 to 1000 mg/kg. Carcinogenicity, immunotoxicity, mutagenicity and cytotoxicity probabilities were also comparatively low in most compounds suggesting that further drug development would be safe (Shulgau et al., 2024). However, compounds A1, A2, and A3 possessed a slightly higher likelihood of being mutagenic; and compounds A3 and A6 a higher likelihood of being cytotoxic. These findings are in accord with other research work done on heterocyclic compounds where low toxicity is usually observed together with good bioavailability. Therefore, even though these compounds look like potential drug candidates (Gummidi et al., 2021).

4.4. Results of Molecular Docking

Table 5: Amino acid, atom from ligand, bond length, bond type, bond category and binding affinities involved in the interaction of 1,3,4-Thiadiazole derivatives.

Compound	Active Amino Residues	Bond Lengths	Bond Category	Bond Type	Docking Score
A1	GLN527, LYS554, ARG560, ASN562, VAL558, PHE559, ILE529, ALA564, LYS512	2.60, 2.97, 3.13, 3.02, 2.51, 3.56, 4.08, 5.09, 5.08, 4.85.22, 4.65, 4.27, 4.91.	Conventional Hydrogen Bond, Carbon Hydrogen Bond, Pi-Donor Hydrogen Bond, Pi-Pi T-shaped, Pi-Alkyl	Hydrogen Bond, Hydrophobic	-7.5
A2	GLN527, ARG560, ASP545,	2.83, 2.91, 2.95, 2.86, 3.50, 5.11,	Conventional Hydrogen Bond, Carbon Hydrogen	Hydrogen Bond, Hydrophobic	-7.9

	VAL558, PHE559, LYS512, ILE529, ALA564	5.28, 5.15, 5.02, 5.05, 4.75, 4.28, 4.89.	Bond, Pi-Pi T-shaped, Pi-Alkyl		
A3	GLN505, THR565, SER511, PHE559, LYS512, LEU504, MET509	3.09, 3.11, 3.01, 3.58, 5.10, 4.20, 5.33, 4.63	Conventional Hydrogen Bond, Carbon Hydrogen Bond, Pi-Pi T-shaped, Pi-Alkyl	Hydrogen Bond, Hydrophobic	-8.5
A4	LYS512, SER511, PRO510, ILE529, PHE559, ARG560	3.16, 3.53, 3.62, 3.95, 5.20, 3.64, 4.98 5.18, 5.23, 4.33.	Conventional Hydrogen Bond, Pi-Sigma, Pi-Pi T-shaped, Pi-Alkyl	Hydrogen Bond, Hydrophobic	-7.1
A5	LYS512, PRO510, PRO475, ASN562, TYR752, TRP629	3.29, 3.67, 4.71, 5.08, 5.33, 4.25, 4.79, 2.70, 3.35, 4.91, 5.20, 4.85, 4.91.	Conventional Hydrogen Bond, Carbon Hydrogen Bond, Amide-Pi Stacked, Pi-Alkyl, Pi-Pi Stacked, Pi-Donor Hydrogen Bond	Hydrogen Bond, Hydrophobic	-6.7
A6	LYS512, THR565, PRO510, PHE559, PRO475, ILE529, ARG560	3.28, 3.27, 3.64, 5.11, 4.74, 3.92, 4.56, 5.11, 5.36, 4.41, 4.92.	Conventional Hydrogen Bond, Carbon Hydrogen Bond, Amide-Pi Stacked, Pi-Pi T-shaped, Pi-Alkyl	Hydrogen Bond, Hydrophobic	-6.6
A7	LYS512 THR565 PRO510 PHE559 PRO475 ILE529 ARG560 PRO475 LYS512 ILE529	3.28, 3.27, 3.64, 5.11, 4.74, 3.92, 4.56, 5.11, 5.36, 4.41, 4.92.	Hydrogen Bond, Hydrophobic	Carbon Hydrogen Bond, Pi-Pi T-shaped, Amide-Pi Stacked, Alkyl, Pi-Alkyl	-6.3
A8	GLU233, ASP197, LYS200, ALA198, TRP59, TYR62, HIS201, ILE235, LEU162	2.96, 5.17, 2.47, 2.77, 2.64, 3.83, 4.06, 4.93, 4.82, 4.45, 3.93, 5.01, 4.86, 4.88, 4.26.	Salt Bridge, Attractive Charge, Conventional Hydrogen Bond, Carbon Hydrogen Bond, Pi-Anion, Pi-Pi Stacked, Pi-Pi T-shaped, Pi-Alkyl	Hydrogen Bond, Hydrophobic	-9.5
A9	LYS512, THR565, PRO510, ARG560,	3.20, 3.33, 3.54, 3.35, 4.65, 5.21,	Conventional Hydrogen Bond, Carbon Hydrogen Bond, Amide-Pi	Hydrogen Bond, Hydrophobic	-7.1

	PRO475, ILE529	5.37, 5.42, 4.48, 4.77.	Stacked, Pi-Alkyl, Halogen		
A10	LYS512, GLN527, LYS554, ARG560, TYR752, ASN562, TRP629	3.02, 3.28, 3.17, 2.95, 3.27, 2.59, 4.52, 4.94, 5.32, 5.27, 4.77, 4.29, 5.47.	Conventional Hydrogen Bond, Pi-Cation, Pi-Anion, Pi-Alkyl	Hydrogen Bond, Hydrophobic	-7.3
NL (Acarbose)	GLN63, TYR151, LYS200, UNL1, THR163, ASP197, GLU233, GLY306, TRP59	2.08, 2.57, 2.38, 2.47, 1.98, 2.02, 2.07, 2.06, 2.67, 4.93, 5.31.	Conventional Hydrogen Bond, Carbon Hydrogen Bond, Pi-Alkyl	Hydrogen Bond, Hydrophobic	-8.1

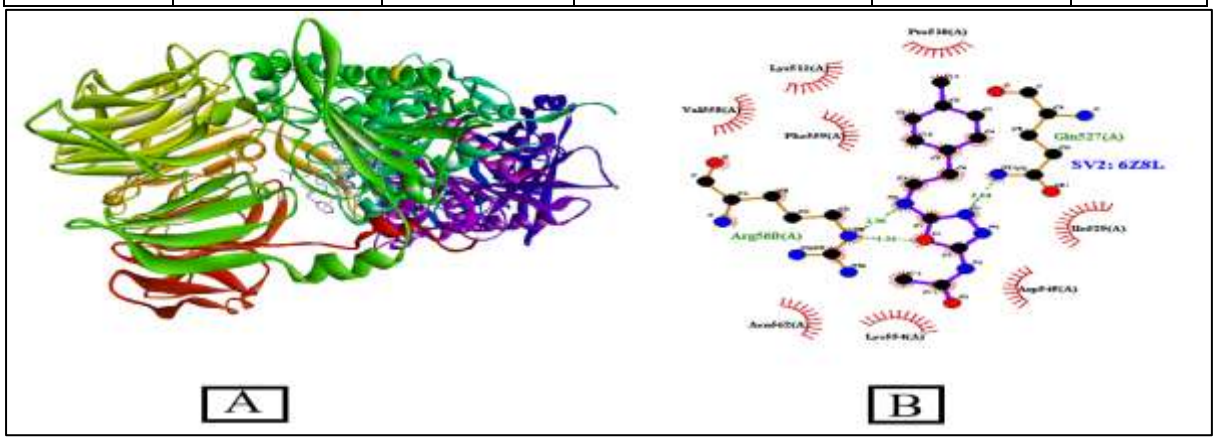

Figure 3: 3D Binding of A2 compound to active site of human pancreatic alpha amylase (PDB ID: 6Z8L) (A) along with the 2D binding diagram (B).

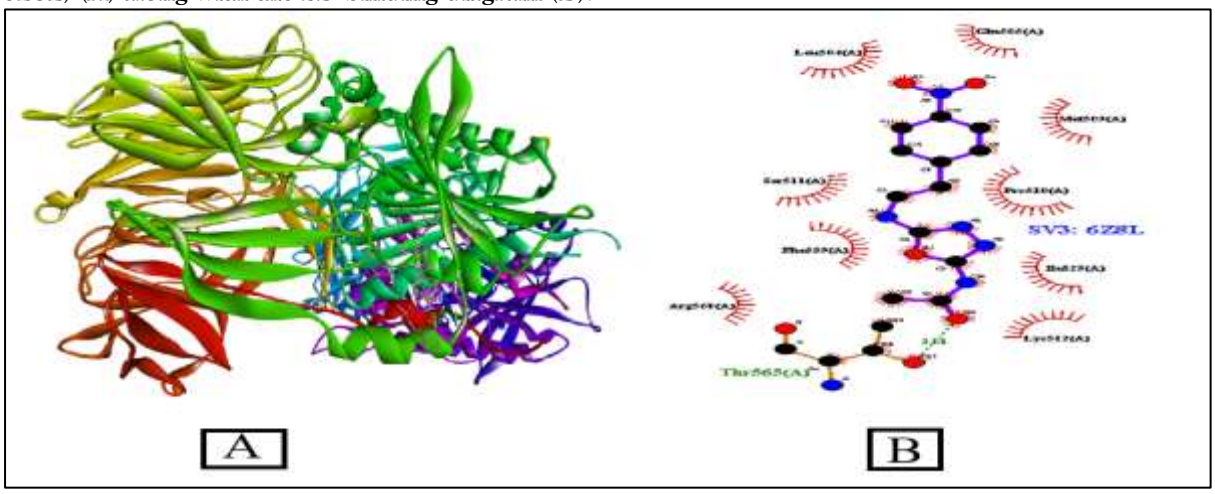

Figure 4: 3D Binding of A3 compound to active site of human pancreatic alpha amylase (PDB ID: 6Z8L) (A) along with the 2D binding diagram (B).

International Journal of Environmental Sciences
ISSN: 2229-7359
Vol. 11 No. 23s, 2025
https://www.theaspd.com/ijes.php

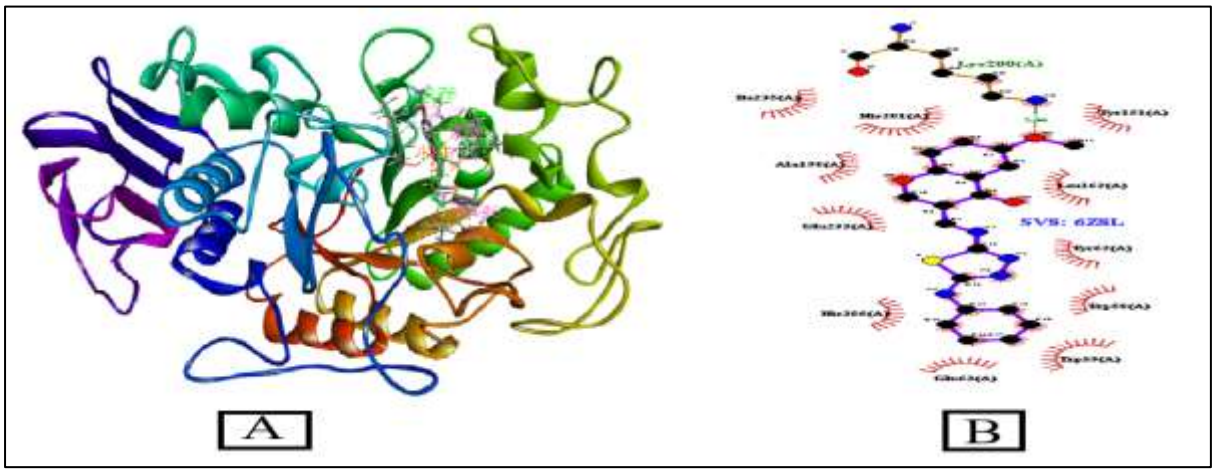

Figure 5: 3D Binding of A8 compound to active site of human pancreatic alpha amylase (PDB ID: 6Z8L) (A) along with the 2D binding diagram (B).

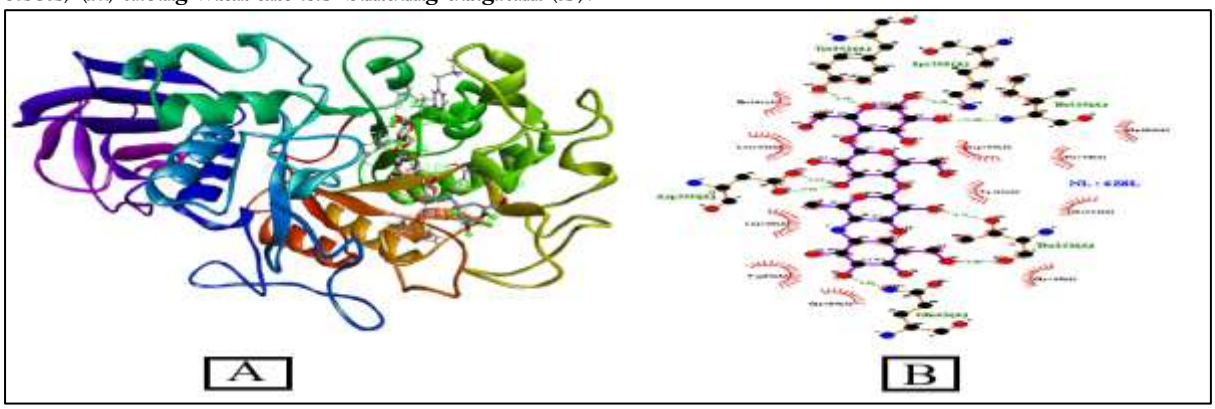

Figure 6: 3D Binding of Native Ligand to active site of human pancreatic alpha amylase (PDB ID: 6Z8L) (A) along with the 2D binding diagram (B).

The molecular docking results of 1,3,4-thiadiazole derivatives revealed promising interactions with the active site of human pancreatic α-amylase, as shown in Table 5. Compounds A1 to A10 exhibited a range of docking scores from -6.3 to -9.5 kcal/mol, with compound A8 showing the best binding affinity at -9.5 kcal/mol. This strong binding was attributed to various key interactions, such as salt bridges and attractive charges, alongside conventional hydrogen bonds and hydrophobic contacts, which were facilitated by active amino residues like GLU233 and ASP197 . In comparison to Acarbose (NL), which had a docking score of -8.1 kcal/mol, the thiadiazole derivatives, especially A8, demonstrated stronger inhibitory potential. Previous studies on heterocyclic inhibitors of α-amylase have reported similar binding patterns, particularly regarding hydrogen bonding and hydrophobic interactions, supporting the findings that these thiadiazole derivatives possess considerable enzyme-inhibitory activity . The 1,3,4-thiadiazole derivatives align well with known enzyme inhibitors, such as thiazolidinediones and benzimidazole derivatives, which also exhibit a combination of hydrogen bonding and hydrophobic interactions with the enzyme active site. For instance, studies by Patel et al. (2020) showed that heterocyclic inhibitors with docking scores around -7.0 kcal/mol displayed effective inhibition of α-amylase. The current results suggest that compounds like A8 and A3, with superior docking scores and strong binding interactions, hold significant potential as potent α-amylase inhibitors, especially considering the favorable engagement with key active site residues and comparable, if not superior, affinity to established inhibitors like Acarbose .
The molecular docking analysis of 1,3,4-thiadiazole derivatives indicated that they have the potential to bind to the active site of human pancreatic α-amylase as given in Table 5. Docking scores for compounds A1 to A10 ranged from -6.3 to -9.5 kcal/mol with compound A8 having the high binding affinity of -9.5 kcal/mol. These included conventional hydrogen bonds and hydrophobic contacts as well as other specific interactions including salt bridges and attractive charges which were made possible by active amino residues including GLU233 and ASP197 (Shulgau et al., 2024). Acarbose (NL) gave a docking score of -8.1 kcal/mol, while the thiadiazole derivatives especially A8 displayed enhanced inhibitory activity. Previous research on heterocyclic inhibitors of α-amylase has also shown similar modes of

binding, especially hydrogen bonding and hydrophobic interactions, which confirms previous findings that these thiadiazole derivatives have good enzyme inhibitory potential (Abbasi et al., 2024). The 1,3,4-thiadiazole derivatives are in good agreement with the known enzyme inhibitors as thiazolidinediones and benzimidazole derivatives, which also have a combination of hydrogen bond and hydrophobic interaction with the active site of enzyme. For instance, Patel et al. (2020) revealed that heterocyclic inhibitors with docking scores of -7.0 kcal/mol had the best inhibition of α-amylase. The present findings indicate that compounds like A8 and A3, which have high docking scores, and strong binding interaction are promising as potent α-amylase inhibitors given the good interaction with active site residues and the comparable or even better binding affinities than Acarbose (Hussain et al., 2022).

The synthesis of 1,3,4-thiadiazole derivatives is quite simple and involves several reflux steps and readily available starting materials including thiosemicarbazide and different substituted anilines. The reaction sequence normally involves the preparation of the intermediate by heating the substituted aniline and thiosemicarbazide in ethanol with formaldehyde, then the addition of NaOH to form the desired heterocyclic thiadiazole ring. The last stage implies the condensation of the synthesized 4H-chromen-3-carbaldehyde with the formed intermediate of thiadiazole to obtain the final compounds. The moderate to high yields (from 67 to 93 percent) and characterized melting points show that the synthesis was successful, and the product is relatively pure. Furthermore, the progress of the reactions was followed up by thin-layer chromatography (TLC), to confirm the completion of each step. The structures of the synthesized compounds are supported by FTIR and NMR spectra. The FTIR spectra of all the synthesized compounds show peaks corresponding to N-H, C-H and C=O stretching and peaks for the different functional groups present in the different derivatives such as aromatic rings, aliphatic chains and halogen atoms (C-Cl and C-F in the case of the corresponding derivatives). The ^{1}H-NMR spectra likewise confirm these observations with the proper chemical shifts for the aromatic, methoxy and the aliphatic protons. These spectroscopic properties are in accordance with earlier findings on some other related thiadiazole-chromone analogs which also display parallel functional group features. Overall the synthetic strategy employed in this study is efficient and scalable, opening up opportunities for future refinements and the synthesis of new members of this compound class.

4.5. Results of *In-vitro* α-amylase inhibitory activity

Table 6: Results of *In-vitro* α-amylase inhibitory activity

Compound	Concentration (µg/mL)	OD at 400 nm (mean ± SD)	Residual activity (mean ± SD, %)	% Inhibition (mean ± SD)
A1	10	0.572±0.073	87.5±2.3	13.5±2.3
	40	0.426±0.068	74.3±1.3	24.7±1.2
	80	0.346±0.034	67.1±1.5	33.9±1.4
	100	0.287±0.051	39.9±1.6	61.1±1.0
A2	10	0.612±0.043	84.3±2.3	16.7±1.3
	40	0.566±0.019	74.4±1.5	39.6±2.2
	80	0.486±0.054	67.3±1.8	52.7±1.2
	100	0.262±0.71	43.7±1.4	86.3±130
A3	10	0.412±0.023	76.5±2.1	24.5±1.1
	40	0.326±0.018	63.3±1.7	37.7±1.7
	80	0.246±0.014	49.1±1.3	51.9±1.3
	100	0.187±0.011	14.9±1.0	87.1±1.0
A4	10	0.512±0.032	86.3±2.7	14.7±1.3
	40	0.475±0.055	77.6±1.4	23.4±1.2
	80	0.355±0.054	61.3±1.3	39.7±1.8
	100	0.262±0.073	44.9±1.3	55.1±0.9
A5	10	0.464±0.083	84.5±1.5	16.5±1.3
	40	0.526±0.078	77.3±1.2	23.7±1.8
	80	0.353±0.069	68.1±1.5	32.9±1.2
	100	0.264±0.064	39.9±1.2	61.1±1.2
A6	10	0.486±0.088	88.8±2.3	12.2±2.2
	40	0.526±0.065	77.6±1.8	23.4±1.1
	80	0.334±0.064	66.3±1.2	34.7±0.9

	100	0.278±0.073	44.9±1.3	56.1±2.2
A7	10	0.546±0.082	87.8±2.3	13.2±2.2
	40	0.486±0.085	71.6±1.6	29.4±2.1
	80	0.364±0.064	66.3±1.9	34.7±1.7
	100	0.288±0.023	44.9±1.9	56.1±2.5
A8	10	0.398±0.021	74.7±2.0	26.3±2.0
	40	0.312±0.017	46.2±1.6	54.8±1.6
	80	0.237±0.013	23.9±1.2	73.1±1.2
	100	0.181±0.010	9.8±0.9	91.2±0.9
A9	10	0.486±0.088	89.8±2.7	11.9±2.2
	40	0.526±0.065	78.6±1.7	22.3±2.1
	80	0.334±0.064	69.3±1.4	31.7±1.2
	100	0.278±0.073	45.9±1.2	55.1±2.5
A10	10	0.619±0.032	82.8±2.3	18.2±1.7
	40	0.579±0.045	69.6±1.8	29.4±1.7
	80	0.453±0.024	61.3±1.8	39.7±1.8
	100	0.343±0.083	37.9±1.9	63.1±1.5
Acarbose	10	0.518±0.028	79.1±2.6	21.9±2.6
	40	0.430±0.024	59.8±2.2	41.2±2.2
	80	0.358±0.020	51.3±1.8	49.7±1.8
	100	0.298±0.016	15.2±1.5	85.8 1.5

Values are expressed in mean±SD (n=3)

Table 7: IC_{50} values for α-amylase inhibition activity of compounds.

Compound	IC_{50} Value (µg/mL)
A1	91.99±1.34
A2	61.54±2.65
A3	59.56±0.87
A4	94.55±1.39
A5	93.43±2.98
A6	97.13±0.29
A7	96.55±1.87
A8	44.67±2.67
A9	101.23±0.98
A10	84.77±1.43
Acarbose	60.51±1.89

Values are expressed in mean±standard deviation (SD)

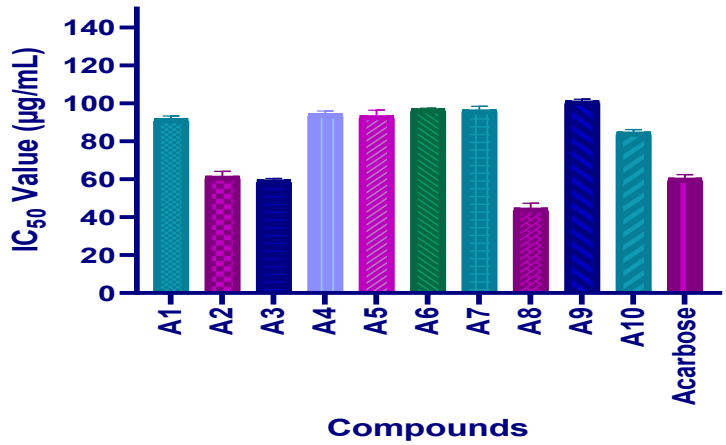

Figure 7: Graphical Representation of IC_{50} Value (µg/mL) of compounds in *In-vitro* α-amylase inhibitory activity

The inhibitory effects of the 1,3,4-thiadiazole derivatives on α-amylase activity are shown in Table 6 and Table 7, which indicate that some of the compounds are more effective than Acarbose in inhibiting α-

amylase activity. Compound A8 had the highest antidiabetic activity with the IC50 of 44.67 µg/mL compared to Acarbose with an IC_{50} of 60.51 µg/mL. At 100 µg/mL of concentration, A8 had the highest inhibition of 91.2% amongst all the compounds tested suggesting that A8 is potent in inhibiting the enzyme at low concentrations. Whereas compounds A2 and A3 also presented considerable inhibition, with IC50 of 61.54 µg/mL and 59.56 µg/mL, respectively, which was close to Acarbose. The remaining compounds A1, A4 and A5 showed moderate to low inhibitory effects with IC50 values varying between 91.99 µg/mL – 93.43 µg/mL (Ali et al., 2024). On comparing the present study with other works done on α-amylase inhibitors, the IC50 values of the 1,3,4-thiadiazole derivatives are in the same range as other heterocyclic compounds (Figure 7). For example, the previous research on thiazolidinediones and benzimidazoles has given IC50 values that are near 50 µg/mL, and this is closely related with the performance of the compound A8, A2 and A3 of this study. Furthermore, the inhibition percentage for some compounds at highest concentration (100 µg/mL) is even higher than that of the standard inhibitors, which proves the potential of these thiadiazole derivatives as α-amylase inhibitors (Zhao et al., 2021). The observed high in-vitro inhibitory activity of these derivatives further validates the therapeutic potential of the strong docking scores [as seen in compounds like A8] indicating that these could be used as potential alternatives or adjuvants to current drugs such as Acarbose in the control of post prandial hyperglycemia in diabetic patients.

CONCLUSION

The synthesis of 1,3,4-thiadiazole derivatives was carried out through the one pot three step reaction sequence and the products were obtained in moderate to good yields as determined by melting point, TLC and spectroscopic analysis using FTIR and ^{1}H NMR. The docking studies showed that compounds A8 and other derivatives had good binding to the active site amino acid residues of α-amylase with favorable docking scores and binding energies. The α-amylase inhibitory activity of the synthesized derivatives further substantiated their possibility to serve as effective enzyme inhibitors than the positive control Acarbose with compound A8 being the most potent. Pharmacokinetic and drug likeness properties showed good absorption by the gastrointestinal tract and low permeability across the blood brain barrier with moderate toxicity. Altogether, these findings indicate that the 1,3,4-thiadiazole derivatives synthesised in this study, with focus on A8, possess great potential for use as α-amylase inhibitors in the treatment of diabetes and should be further evaluated in preclinical trials.

Abbreviations

GI – Gastrointestinal; BBB - Blood-Brain Barrier; P-gp - P-glycoprotein; CYP - Cytochrome P450; LD50 - Lethal Dose, 50%; HBD - Hydrogen Bond Donor; HBA - Hydrogen Bond Acceptor; Mol. Wt. - Molecular Weight; Log P - Partition Coefficient; TPSA - Total Polar Surface Area; ADMET - Absorption, Distribution, Metabolism, Excretion, and Toxicity; Log Kp - Logarithm of Skin Permeation Coefficient. FTIR: Fourier-transform infrared spectroscopy; NMR: nuclear magnetic resonance spectroscopy; MS: mass spectrometry; TMS: tetramethylsilane; TLC: Thin-layer chromatography; DMSO: Dimethyl sulfoxide.

Authors Contribution

Vijay V. Pawar- Conceptualization, Study design, Software, Validation, Investigation, Resources, Writing – original draft, **Sandip G. Badadhe**- Formal analysis, Data curation, Visualization, Writing – review and editing, Visualization, **Swati B. Fulsundar**- Writing – review and editing, Visualization.

REFERENCES

1. Abbasi, S. A., Rahim, F., Hussain, R., Khan, S., Ullah, H., Iqbal, T., Iqbal, N., Khan, H. U., Khan, S., Iqbal, R., Shah, S. A. A., Al Obaid, S., & Ansari, M. J. (2024). Synthesis of modified 1,3,4-thiadiazole incorporating substituted thiosemicarbazide derivatives: Elucidating the *in vitro* and *in silico* studies to develop promising anti-diabetic agent. *Results in Chemistry*, *8*, 101556. https://doi.org/10.1016/j.rechem.2024.101556
2. Agrwal, A., Pathak, R. K., & Kasana, V. (2022). Molecular Docking and Antibacterial Studies of Pyranopyrazole Derivatives Synthesized Using [Pap-Glu@Chi] Biocatalyst Through a Greener Approach. *Arabian Journal for Science and Engineering*, *47*(1), 347–363. https://doi.org/10.1007/s13369-021-05377-1
3. Ali, Z., Rehman, W., Rasheed, L., Alzahrani, A. Y., Ali, N., Hussain, R., Emwas, A.-H., Jaremko, M., & Abdellattif, M. H. (2024). New 1,3,4-Thiadiazole Derivatives as α-Glucosidase Inhibitors: Design, Synthesis, DFT, ADME, and In Vitro Enzymatic Studies. *ACS Omega*, *9*(7), 7480–7490. https://doi.org/10.1021/acsomega.3c05854
4. Aliabadi, A. (2016). 1,3,4-Thiadiazole Based Anticancer Agents. *Anti-Cancer Agents in Medicinal Chemistry- Anti-Cancer Agents)*, *16*(10), 1301–1314.
5. Anthwal, T., Paliwal, S., & Nain, S. (2022). Diverse Biological Activities of 1,3,4-Thiadiazole Scaffold. *Chemistry*, *4*(4), Article 4. https://doi.org/10.3390/chemistry4040107

6. Asmat, U., Abad, K., & Ismail, K. (2016). Diabetes mellitus and oxidative stress—A concise review. *Saudi Pharmaceutical Journal*, *24*(5), 547–553. https://doi.org/10.1016/j.jsps.2015.03.013
7. Banerjee, P., Eckert, A. O., Schrey, A. K., & Preissner, R. (2018). ProTox-II: A webserver for the prediction of toxicity of chemicals. *Nucleic Acids Research*, *46*(W1), W257–W263. https://doi.org/10.1093/nar/gky318
8. Banerjee, P., & Ulker, O. C. (2022). Combinative ex vivo studies and in silico models ProTox-II for investigating the toxicity of chemicals used mainly in cosmetic products. *Toxicology Mechanisms and Methods*, *32*(7), 542–548. https://doi.org/10.1080/15376516.2022.2053623
9. Bhongade, B. A., Talath, S., Gadad, R. A., & Gadad, A. K. (2016). Biological activities of imidazo[2,1-b][1,3,4]thiadiazole derivatives: A review. *Journal of Saudi Chemical Society*, *20*, S463–S475. https://doi.org/10.1016/j.jscs.2013.01.010
10. Butt, S. S., Badshah, Y., Shabbir, M., & Rafiq, M. (2020). Molecular Docking Using Chimera and Autodock Vina Software for Nonbioinformaticians. *JMIR Bioinformatics and Biotechnology*, *1*(1), e14232. https://doi.org/10.2196/14232
11. Chavan, S. U., Waghmare, S. A., Bodke, S. S., & Bendale, A. R. (2023). Exploring 1,3,4-Oxadiazole Derivatives as Potent α-Amylase Inhibitors: Design, Synthesis, and Biological Evaluation. *EURASIAN JOURNAL OF CHEMISTRY*, *28*(4 (112)), Article 4 (112). https://doi.org/10.31489/2959-0663/4-23-7
12. Che, X., Liu, Q., & Zhang, L. (2023). An accurate and universal protein-small molecule batch docking solution using Autodock Vina. *Results in Engineering*, *19*, 101335. https://doi.org/10.1016/j.rineng.2023.101335
13. Cole, J. B., & Florez, J. C. (2020). Genetics of diabetes mellitus and diabetes complications. *Nature Reviews Nephrology*, *16*(7), 377–390. https://doi.org/10.1038/s41581-020-0278-5
14. Di Muzio, E., Toti, D., & Polticelli, F. (2017). DockingApp: A user friendly interface for facilitated docking simulations with AutoDock Vina. *Journal of Computer-Aided Molecular Design*, *31*(2), 213–218. https://doi.org/10.1007/s10822-016-0006-1
15. Dou, C. N. D., Dembele, G. S., Kone, M. G.-R., Tuo, N. T., Konate, F., Niare, A., Karamanis, P., & Ziao, N. (2023). Design of New Thiadiazole Derivatives with Improved Antidiabetic Activity. *Computational Chemistry*, *11*(03), 67–80. https://doi.org/10.4236/cc.2023.113005
16. El-Hachem, N., Haibe-Kains, B., Khalil, A., Kobeissy, F. H., & Nemer, G. (2017). AutoDock and AutoDockTools for Protein-Ligand Docking: Beta-Site Amyloid Precursor Protein Cleaving Enzyme 1(BACE1) as a Case Study. In F. H. Kobeissy & Jr. Stevens Stanley M. (Eds.), *Neuroproteomics: Methods and Protocols* (pp. 391–403). Springer. https://doi.org/10.1007/978-1-4939-6952-4_20
17. Forli, S., Huey, R., Pique, M. E., Sanner, M. F., Goodsell, D. S., & Olson, A. J. (2016). Computational protein–ligand docking and virtual drug screening with the AutoDock suite. *Nature Protocols*, *11*(5), 905–919. https://doi.org/10.1038/nprot.2016.051
18. Gummidi, L., Kerru, N., Ebenezer, O., Awolade, P., Sanni, O., Islam, Md. S., & Singh, P. (2021). Multicomponent reaction for the synthesis of new 1,3,4-thiadiazole-thiazolidine-4-one molecular hybrids as promising antidiabetic agents through α-glucosidase and α-amylase inhibition. *Bioorganic Chemistry*, *115*, 105210. https://doi.org/10.1016/j.bioorg.2021.105210
19. Hussain, R., Shah, M., Iqbal, S., Rehman, W., Khan, S., Rasheed, L., Naz, H., Al-ghulikah, H. A., Elkaeed, E. B., Pashameah, R. A., Alzahrani, E., & Farouk, A.-E. (2022). Molecular iodine-promoted oxidative cyclization for the synthesis of 1,3,4-thiadiazole-fused- [1,2,4]-thiadiazole incorporating 1,4-benzodioxine moiety as potent inhibitors of α-amylase and α-glucosidase: In vitro and in silico study. *Frontiers in Chemistry*, *10*. https://doi.org/10.3389/fchem.2022.1023316
20. Janowska, S., Khylyuk, D., Bielawska, A., Szymanowska, A., Gornowicz, A., Bielawski, K., Noworól, J., Mandziuk, S., & Wujec, M. (2022). New 1,3,4-Thiadiazole Derivatives with Anticancer Activity. *Molecules*, *27*(6), Article 6. https://doi.org/10.3390/molecules27061814
21. Janowska, S., Paneth, A., & Wujec, M. (2020). Cytotoxic Properties of 1,3,4-Thiadiazole Derivatives—A Review. *Molecules*, *25*(18), Article 18. https://doi.org/10.3390/molecules25184309
22. Johns, E. C., Denison, F. C., Norman, J. E., & Reynolds, R. M. (2018). Gestational Diabetes Mellitus: Mechanisms, Treatment, and Complications. *Trends in Endocrinology & Metabolism*, *29*(11), 743–754. https://doi.org/10.1016/j.tem.2018.09.004
23. Kashtoh, H., & Baek, K.-H. (2023). New Insights into the Latest Advancement in α-Amylase Inhibitors of Plant Origin with Anti-Diabetic Effects. *Plants*, *12*(16), Article 16. https://doi.org/10.3390/plants12162944
24. Katsarou, A., Gudbjörnsdottir, S., Rawshani, A., Dabelea, D., Bonifacio, E., Anderson, B. J., Jacobsen, L. M., Schatz, D. A., & Lernmark, Å. (2017). Type 1 diabetes mellitus. *Nature Reviews Disease Primers*, *3*(1), 1–17. https://doi.org/10.1038/nrdp.2017.16
25. Kaur, N., Kumar, V., Nayak, S. K., Wadhwa, P., Kaur, P., & Sahu, S. K. (2021). Alpha-amylase as molecular target for treatment of diabetes mellitus: A comprehensive review. *Chemical Biology & Drug Design*, *98*(4), 539–560. https://doi.org/10.1111/cbdd.13909
26. Kontoyianni, M. (2017). Docking and Virtual Screening in Drug Discovery. In I. M. Lazar, M. Kontoyianni, & A. C. Lazar (Eds.), *Proteomics for Drug Discovery: Methods and Protocols* (pp. 255–266). Springer. https://doi.org/10.1007/978-1-4939-7201-2_18
27. Li, X., Bai, Y., Jin, Z., & Svensson, B. (2022). Food-derived non-phenolic α-amylase and α-glucosidase inhibitors for controlling starch digestion rate and guiding diabetes-friendly recipes. *LWT*, *153*, 112455. https://doi.org/10.1016/j.lwt.2021.112455
28. Mahmood, N. (2016). A review of α-amylase inhibitors on weight loss and glycemic control in pathological state such as obesity and diabetes. *Comparative Clinical Pathology*, *25*(6), 1253–1264. https://doi.org/10.1007/s00580-014-1967-x
29. McIntyre, H. D., Catalano, P., Zhang, C., Desoye, G., Mathiesen, E. R., & Damm, P. (2019). Gestational diabetes mellitus. *Nature Reviews Disease Primers*, *5*(1), 1–19. https://doi.org/10.1038/s41572-019-0098-8
30. Othman, A. A., Kihel, M., & Amara, S. (2019). 1,3,4-Oxadiazole, 1,3,4-thiadiazole and 1,2,4-triazole derivatives as potential antibacterial agents. *Arabian Journal of Chemistry*, *12*(7), 1660–1675. https://doi.org/10.1016/j.arabjc.2014.09.003

31. Proença, C., Ribeiro, D., Freitas, M., & Fernandes, E. (2022). Flavonoids as potential agents in the management of type 2 diabetes through the modulation of α-amylase and α-glucosidase activity: A review. *Critical Reviews in Food Science and Nutrition*, *62*(12), 3137–3207. https://doi.org/10.1080/10408398.2020.1862755
32. Rasouli, H., Hosseini-Ghazvini, S. M.-B., Adibi, H., & Khodarahmi, R. (2017). Differential α-amylase/α-glucosidase inhibitory activities of plant-derived phenolic compounds: A virtual screening perspective for the treatment of obesity and diabetes. *Food & Function*, *8*(5), 1942–1954. https://doi.org/10.1039/C7FO00220C
33. Shulgau, Z., Palamarchuk, I. V., Sergazy, S., Urazbayeva, A., Ramankulov, Y., & Kulakov, I. V. (2024). Synthesis, Computational Study, and In Vitro α-Glucosidase Inhibitory Action of 1,3,4-Thiadiazole Derivatives of 3-Aminopyridin-2(1H)-ones. *Pharmaceuticals*, *17*(3), Article 3. https://doi.org/10.3390/ph17030377
34. Taha, M., Khan, A. A., Rahim, F., Hayat, S., Imran, S., Iqbal, N., Uddin, N., Khan, K. M., Anouar, E. H., Farooq, R. K., Nawaz, M., & Shah, S. A. A. (2023). Synthesis, in vitro evaluation and molecular docking studies of hybrid 4-quinolinyl bearing 1,3,4-thiadiazole-2-amine as a new inhibitor of α-amylase and α-glucosidase. *Journal of Molecular Structure*, *1282*, 135173. https://doi.org/10.1016/j.molstruc.2023.135173
35. Tanchuk, V. Y., Tanin, V. O., Vovk, A. I., & Poda, G. (2016). A New, Improved Hybrid Scoring Function for Molecular Docking and Scoring Based on AutoDock and AutoDock Vina. *Chemical Biology & Drug Design*, *87*(4), 618–625. https://doi.org/10.1111/cbdd.12697
36. Teng, H., & Chen, L. (2017). α-Glucosidase and α-amylase inhibitors from seed oil: A review of liposoluble substance to treat diabetes. *Critical Reviews in Food Science and Nutrition*, *57*(16), 3438–3448. https://doi.org/10.1080/10408398.2015.1129309
37. Tomic, D., Shaw, J. E., & Magliano, D. J. (2022). The burden and risks of emerging complications of diabetes mellitus. *Nature Reviews Endocrinology*, *18*(9), 525–539. https://doi.org/10.1038/s41574-022-00690-7
38. Tripathi, A., & Misra, K. (2017). Molecular Docking: A Structure-Based Drug Designing Approach. *JSM Chemistry*, *5*.
39. Unnikrishnan, R., Anjana, R. M., & Mohan, V. (2016). Diabetes mellitus and its complications in India. *Nature Reviews Endocrinology*, *12*(6), 357–370. https://doi.org/10.1038/nrendo.2016.53
40. Valdés-Tresanco, M. S., Valdés-Tresanco, M. E., Valiente, P. A., & Moreno, E. (2020). AMDock: A versatile graphical tool for assisting molecular docking with Autodock Vina and Autodock4. *Biology Direct*, *15*(1), 12. https://doi.org/10.1186/s13062-020-00267-2
41. Yang, C., Chen, E. A., & Zhang, Y. (2022). Protein–Ligand Docking in the Machine-Learning Era. *Molecules*, *27*(14), Article 14. https://doi.org/10.3390/molecules27144568
42. Ya'u Ibrahim, Z., Uzairu, A., Shallangwa, G., & Abechi, S. (2020). Molecular docking studies, drug-likeness and *in-silico* ADMET prediction of some novel β-Amino alcohol grafted 1,4,5-trisubstituted 1,2,3-triazoles derivatives as elevators of p53 protein levels. *Scientific African*, *10*, e00570. https://doi.org/10.1016/j.sciaf.2020.e00570
43. Zhao, X., Zhan, X., Zhang, H., Wan, Y., Yang, H., Wang, Y., Chen, Y., & Xie, W. (2021). Synthesis and biological evaluation of isatin derivatives containing 1,3,4-thiadiazole as potent a-glucosidase inhibitors. *Bioorganic & Medicinal Chemistry Letters*, *54*, 128447. https://doi.org/10.1016/j.bmcl.2021.128447